

DKK1/SMDT1 participate in Ang II-induced mitochondrial injury of human smooth muscle cells in an abdominal aortic aneurysm cell model

XIAOXIA CHANG^{1*}, BAOHONG YAO^{2*}, ZHENG LIU^{3*}, ZIJIE GUO⁴,
PENGYUE QIAO⁴, XIAOKUN LI³, LIN WANG⁵ and AIQUN LI³

¹Department of Cardiology, Muping Hospital of Traditional Chinese Medicine, Yantai, Shandong 264100, P.R. China; ²Department of Cardiac Surgery, Yantai Affiliated Hospital of Binzhou Medical University, Yantai, Shandong 264100, P.R. China; ³Department of Emergency Surgery, Yantai Affiliated Hospital of Binzhou Medical University, Yantai, Shandong 264100, P.R. China; ⁴Department of Introduction to Medicine, School of Basic Medical Sciences, Binzhou Medical University, Yantai, Shandong 264100, P.R. China; ⁵Department of Cardiology, Central Hospital Affiliated to Shandong First Medical University, Jinan, Shandong 250000, P.R. China

Received March 21, 2025; Accepted November 5, 2025

DOI: 10.3892/etm.2026.13112

Abstract. Abdominal aortic aneurysm (AAA) is a lethal vascular disease, in which apoptosis and inflammation participate. However, the regulatory factors associated with aortic status remain unclear; therefore, a deeper understanding of the cell types and signaling pathways involved in the pathological process of AAAs is key to the development of medical treatments. The aim of the present study was to explore the role of dickkopf-1 (DKK1) in angiotensin (Ang) II-stimulated human smooth muscle cells (HSMCs), and to clarify the potential downstream targets and related pathological mechanisms of DKK1. HSMCs were stimulated with Ang II (1 μ M) for 24 h; consequently, DKK1 protein expression was upregulated by 4.26-fold and increased mRNA expression levels of IL-1 β , GRP-94 and GRP-78 were also observed, indicating mitochondrial and endoplasmic reticulum stress. DKK1 silencing

via small interfering RNA reduced its expression, which was validated by reverse transcription-quantitative PCR. RNA sequencing was performed in four groups: Negative control (NC), siDKK1, NC-Ang II and siDKK1-Ang II. Differentially expressed genes (DEGs) were identified by DESeq2, and 1,332 co-expressed DEGs were revealed by Venn analysis, enriched in pathways, including 'protein processing in the endoplasmic reticulum'. Robust rank aggregation prioritized key genes, notably single-pass membrane protein with aspartate rich tail 1 (SMDT1), a mitochondrial calcium regulator. The mRNA of SMDT1 was upregulated by Ang II stimulation by 2.78-fold, which was reversed by DKK1 silencing by 0.37-fold. Functional enrichment associated DEGs to viral response, extracellular matrix and cytokine pathways. Protein-protein interaction networks highlighted gene clusters via STRING. In conclusion, the present study investigated the role of DKK1 in Ang II-induced mitochondrial dysfunction in HSMCs. To the best of our knowledge, the present study demonstrated, for the first time, that DKK1/SMDT1 mediated Ang II-induced mitochondrial injury in HSMCs, suggesting this pathway as a potential mechanism. Therefore, the results indicated that DKK1 could serve as a therapeutic target for the prevention of AAA.

Correspondence to: Professor Aiqun Li, Department of Emergency Surgery, Yantai Affiliated Hospital of Binzhou Medical University, 717 Jinbu Street, Yantai, Shandong 264100, P.R. China
E-mail: byjzkw@126.com

Professor Lin Wang, Department of Cardiology, Central Hospital Affiliated to Shandong First Medical University, 10 Jiefang Road, Jinan, Shandong 250000, P.R. China
E-mail: wanglin54202003@163.com

*Contributed equally

Abbreviations: AAA, abdominal aortic aneurysm; VSMCs, vascular smooth muscle cells; Ang, angiotensin; Wnt/ β -catenin, Wingless/beta catenin; DKK1, dickkopf-1; SMDT1, single-pass membrane protein with aspartate rich tail 1; RRA, robust rank aggregation; MCU, mitochondrial calcium uniporter

Key words: DKK1, mitochondrial injury, SMDT1, angiotensin II, abdominal aortic aneurysm

Introduction

Abdominal aortic aneurysm (AAA), defined as the regional enlargement of the abdominal aorta to a diameter of >50% greater compared with its adjacent healthy size or an aorta that measures >30 mm in diameter (1,2), is a key cause of mortality among individuals aged >65 years, due to rupture of the dilation aorta tissue. In addition, the mortality rate of patients with AAA is >80% following rupture, despite surgical advancements (3). Effective pharmacotherapies for halting the growth and rupture of AAA or delaying the requirement for surgical repair are lacking at present.

The pathogenesis of vascular injury in aortic aneurysms involves the apoptosis of vascular smooth muscle cells

(VSMCs) and the enhancement of extracellular matrix metalloproteinase (MMP) activity, oxidative stress aggravated by endothelial cell dysfunction and the increase of inflammatory cell infiltration in the vascular wall. At present, mitochondrial dysfunction is considered to carry out a vital role in the development of AAA; results of a previous study using single-cell RNA sequencing demonstrated that excessive mitochondrial dysfunction occurs in different aortic cell types and is a key character of aortic aneurysms (4). The regulation of mitochondrial metabolism in VSMCs is involved in the pathogenesis of AAA (5,6); VSMCs derived from patients with AAA exhibited increased mitochondrial fragmentation, elevated reactive oxygen species (ROS) production and DNA damage, highlighting the role of mitochondrial health in AAA progression (7). In addition, results of a previous study demonstrated that angiotensin II (Ang II) induced mitochondrial dysfunction in VSMCs, contributing to AAA development; consequently, restoring mitochondrial function in VSMCs attenuated AAA formation in mice models infused with Ang II, emphasizing the therapeutic potential of targeting mitochondrial pathways (8).

Wingless/ β catenin (Wnt/ β -catenin) signaling is often involved in the pathological progression of vascular diseases associated with endothelial dysfunction, proliferation (9), macrophage activation (10) and VSMC migration (11). Moreover, Wnt/ β -catenin signaling was involved not only in chronic kidney disease-associated vascular calcification (12), but also in the osteogenic conversion of VSMCs (13). Through forming a complex with receptors, such as LRP5/6 and Kremen, in the cell membrane, Dickkopf-1 (DKK1) inhibited Wnt/ β -catenin signaling (14). Results of a prospective, population-based clinical cohort study revealed that elevated baseline levels of DKK1 were independently associated with the occurrence of cardiovascular events, providing clinical implications for investigating its role in the pathogenesis of cardiovascular disease (15). Notably, numerous investigations have highlighted the association between elevated plasma levels of DKK1 and the presence of cardiovascular diseases (16,17). DKK1 was involved in vascular calcification, endothelial cell interstitial transformation and mitochondrial disorder in vascular endothelial cells (18). However, it is still unknown whether DKK1 is involved in the regulation of AAA.

While DKK1 is primarily recognized for its role in Wnt signaling, emerging evidence suggests involvement in mitochondrial regulation (18). However, the specific interaction between DKK1 and single-pass membrane protein with aspartate rich tail 1 (SMDT1), a component of the mitochondrial calcium uniporter (MCU) complex, in the context of Ang II-induced mitochondrial injury in VSMCs, is novel and not extensively explored in current literature. The present study explored whether DKK1/SMDT1 mediated Ang II-induced mitochondrial injury in primary cultured HSMCs, thereby clarifying DKK1 whether could serve as a therapeutic target for the prevention of AAA.

Materials and methods

Cell culture and treatment. Passage 2 human aortic smooth muscle cells (HSMCs; cat. no. CP-H081; <https://www.procell.com.cn/p/human-aortic-smooth-muscle-cells-cp-h081-69769>;

Procell Life Science & Technology Co., Ltd.) which carried the SV40T gene were used in the present study. Cells from passages 4 to 10 were cultured in smooth muscle cell medium (cat. no. 1101; ScienCell Research Laboratories, Inc.) in a 5% CO₂ incubator at 37°C. HSMCs were stimulated by human Ang II (1 μ M; cat. no. HY-13948; MedChemExpress) for 24 h; the concentration of Ang II was chosen based on a previous study (19). The HSMCs isolated by Procell laboratory were identified by immunofluorescence for α -SMA, with a purity of >90%, and free of HIV-1, HBV, HCV, mycoplasma, bacteria, yeast and fungi (data not shown).

Western blot assay. Cell homogenates were lysed in an ice-cold radioimmunoprecipitation lysis buffer (cat. no. AR0102; Wuhan Boster Biological Technology Co., Ltd.) with 1 mM phenylmethanesulphonyl fluoride (liquid, 100x, cat. no. AR1192; Wuhan Boster Biological Technology Co., Ltd.) and then the total protein concentration was measured by a BCA protein concentration kit (cat. no. P0010; ProteinTech Group, Inc.). Protein extracts (30 μ g per lane) were loaded and separated by 8-12% SDS-PAGE and transferred to a PVDF membrane (cat. no. IPVH00010; MilliporeSigma). Next the membranes were blocked in 5% skimmed milk powder for 15 min at room temperature (RT), and then were incubated with primary antibodies at 4°C overnight; the primary antibodies included anti-DKK1 (1:1,000; cat. no. ab109416; Abcam) and GAPDH (1:5,000; cat. no. 60004-1-Ig; ProteinTech Group, Inc.). Membranes were then incubated with secondary antibodies at RT for 2 h the next day and included HRP-conjugated Affinipure Goat Anti-Mouse IgG (H+L), (1:5,000; cat. no. SA00001-1; ProteinTech Group, Inc.) and HRP-conjugated Affinipure Goat Anti-Rabbit IgG (H+L) (1:10,000; cat. no. ZB-2301; Beijing Zhongshan Jinqiao Biotechnology Co., Ltd.). The bands were exposed using Tanon5200 (Tanon Science and Technology Co., Ltd.). Densitometry analysis was performed for semi-quantification using ImageJ 1.53t software (National Institutes of Health), using GAPDH as the internal control. The experiments were performed in triplicate.

RNA extraction and reverse transcription-quantitative PCR (RT-qPCR). Total RNA was isolated from HSMCs using an Ultrapure RNA Kit (cat. no. CW0581S; Jiangsu CoWin Biotech Co., Ltd.) according to the manufacturer's instructions and then converted to cDNA using an Evo M-MLV RT Master Mix (cat. no. AG11706; Accurate Biology Co., Ltd.) at 37°C for 15 min and 85°C for 5 sec. After RT, qPCR was performed with a CFX connect Real-Time PCR System (Bio-Rad Laboratories, Inc.) using SYBR Green Pro Taq HS Premix (cat. no. AG11701; Accurate Biology Co., Ltd.). The thermocycling conditions were 95°C for 5 sec and then 60°C for 30 sec for 40 cycles, following a step at 95°C for 30 sec. GAPDH was the internal control, and the primer sequences are provided in Table I. The relative fold change was quantified using the 2^{- $\Delta\Delta$ C_t} method (20); the experiments were performed in triplicate.

Transfection of HSMCs with small interfering RNA (siRNA) and vector. siRNAs targeting human DKK1 (5'-GCUUCA

Table I. PCR primer sequences.

Gene	Accession no.	Forward primer (5' to 3')	Reverse primer (5' to 3')
Human DKK1	NM_012242.4	AGGCACGCTATGTGCTG	CAGTGTGGTTCTTCTGGGA
Human IL-1 β	NM_000576.3	AGCACCTTCTTTCCCTTCATCTT	CACCACTTGTGTGCTCCATATCCT
Human GRP-78	NM_005347.5	TATTGGAGGTGGGCAAACAAAGA	CAGCAATAGTTCAGCGTCTTTG
Human GRP-94	NM_003299.3	TGACAGAATCTCCGTGTGCTTTG	CAGCGGGTGTCTGGGATTAATTT
Human SMDT1	NM_033318.5	TCTCCGTGTGTTCTCCATTGT	TAGTCATCATCATCATCCTCTG
Human GAPDH	NM_002046.7	GGTGAAGGTCGGTGTGAACG	CTCGCTCCTGGAAGATGGTG

CACUUGUCAGAGATT-3') with a high silencing efficiency and scrambled siRNAs as negative control (NC) were purchased from Changzhou Ruibo Bio-Technology Co., Ltd. When HSMCs reached 70-80% confluence, they were transfected with these siRNAs (50 nM) using Lipofectamine RNAi MAX (Invitrogen; Thermo Fisher Scientific, Inc.) according to the manufacturer's instructions. After the 6 h of transfection at 37°C, the medium was replaced with smooth muscle cell medium. Sufficiently downregulated expression caused by these siRNAs was verified by RT-qPCR 48 h after transfection. The scrambled siRNAs were used as controls across all steps.

RNA sequencing (RNA-seq). Total RNA was extracted from each group of HSMCs transfected with siRNA using the VAMNE Magnetic Universal Total RNA Kit (cat. no. ROA3301; Vazyme Biotech Co., Ltd.). The purity of RNA samples was detected by NanoPhotometer® NP80 ultramicro spectrophotometer (Implen GmbH). The concentration of RNA samples was detected by Qubit®3.0 Fluorometer (Life Technologies; Thermo Fischer Scientific, Inc.). The integrity of RNA samples was determined by the Agilent 2100 RNA Nano 6000 Assay Kit (Agilent Technologies, Inc.). After the total RNA samples were qualified, the mRNAs were purified by poly-A selection and rRNA depletion and the library was constructed. The loading concentration of the final library was 20 pM, as measured by iQ™ SYBR® Green Supermix (cat. no. 1708882; Bio-Rad Laboratories, Inc.) on a CFX 96 Real-Time PCR System (Bio-Rad Laboratories, Inc.) The sequencing was performed using a NovaSeq 6000 S4 Reagent Kit V1.5 (cat. no. 20028312; Illumina, Inc.) using Next Generation Sequencing on an Illumina NovaSeq (Illumina, Inc.) sequencing platform. The nucleotide length was 150 bp and the direction of sequencing was paired end. Raw sequencing data were transformed to FastQ format, and the FastQ files were checked for quality assessment by FastQC (v0.11.7; <http://www.bioinformatics.babraham.ac.uk/projects/fastqc>). The Phred Quality Score (Q) of 30 indicates that the base sequencing error rate is 0.1%. Q30 percentage >85% indicates that the sequencing quality is up to standard. The data were filtered by removal of adaptor sequences and low-quality reads in order to get the clean data; the adaptor sequences (the minimum required adapter overlap/stringency: 5bp) and low quality reads (the cutoff of Q value=19) were removed by Trim Galore software (v 0.6.1;

https://www.bioinformatics.babraham.ac.uk/projects/trim_galore/) and Cutadapt (21). The duplicate sequences were not removed, because removing duplicates might lead to the loss of important biological information, especially for highly expressed genes (22). Before analysis, the sequence was aligned, and the abundance of transcripts was quantified; the clean data was aligned to the GRCh38 human reference genome in Ensemble (<http://www.ensembl.org/index.html>) using HISAT2 (v2.1.0.; <https://github.com/DaehwanKimLab/hisat2>). Reads count for each gene in each sample was counted by HTSeq (v2.0.0, <https://htseq.readthedocs.io/en/latest/>) and FPKM (fragments per kilobase million mapped reads) was then calculated to estimate the expression level of genes in each sample. There were four groups from different experimental conditions for HSMCs with two biological replicates in each group: Negative control (NC), siDKK1, NC-Ang II and siDKK1-Ang II. The experimental groups were based on previously published research (18).

Differentially expressed gene (DEG) analysis. DESeq2 (v1.20.0; <https://www.bioconductor.org/packages/devel/bioc/html/DESeq2.html>) was used to analyze the expression of DEGs, and the fold change value and adjusted P-value were used as the main indicators. \log_2 fold change ≥ 1 and adjusted P-value <0.05 were selected as the thresholds. The results of DEG analysis were visualized using the 'ggplot2' R package (v4.2.1; <https://cran.r-project.org/package=ggplot2>) (23).

Venn diagram analysis. Overlapping genes between each group of data were visualized using the 'ggplot2' R package and the 'VennDiagram' R package (v1.7.3; <https://CRAN.R-project.org/package=VennDiagram>) (24).

Robust rank aggregation (RRA) analysis. RRA algorithm was used to sort and merge multiple data sets, to screen out the key genes from the DEGs and visualize them in the form of heat maps using the 'RobustRankAggreg' R package (v1.2.1; <https://CRAN.R-project.org/package=RobustRankAggreg>) (25) and the 'ggplot2' R package.

Functional enrichment analysis. Gene Ontology (GO; <https://geneontology.org>) and Kyoto Encyclopedia of Genes and Genomes (KEGG; <https://www.kegg.jp>) pathway enrichment analysis of the screened genes were performed using the

'clusterProfiler' R package (v4.2.0; <https://www.bioconductor.org/packages/devel/bioc/html/clusterProfiler.html>) (26). The adjusted $P < 0.05$ was set as the cut-off criterion.

Protein-protein interaction (PPI) network analysis. STRING (<https://string-db.org/>) database was utilized to analyze the PPI data. Firstly, the 'multiple proteins' option was selected and the genes in the top 60 RRA scores were then input into the STRING database (27), and 'Homo sapiens' was selected in the species option. The obtained PPI data were illustrated into a high-level network diagram using the 'igraph' R package (v1.4.0; <https://cran.r-project.org/web/packages/igraph/index.html>) and the 'ggraph' R package (v2.2.0; <https://cran.r-project.org/web/packages/ggraph/index.html>).

Statistical analysis. The data in the *in vitro* experiments are presented as the mean \pm SE from three independent experiments. The statistical analysis was performed by unpaired student's t-tests or two-way ANOVA followed by post hoc Tukey's multiple comparisons test in Figs. 2B and 5F using GraphPad Prism 9.4 software (Dotmatics). $P < 0.05$ was considered to indicate a statistically significant difference. Benjamini-Hochberg multiple corrections were applied in DEG analysis.

Results

Ang II promotes DKK1 expression and mitochondrial damage-associated mRNAs in HSMCs. HSMCs were stimulated with 1 μM /l Ang II for 24 h. Results of the western blot analysis revealed that DKK1 protein expression was significantly increased by 4.26-fold in HSMCs following Ang II stimulation (Fig. 1A). Furthermore, mRNA expression levels of IL-1 β and mitochondrial damage-associated genes, GRP-94 and GRP-78, were significantly increased in HSMCs following Ang II stimulation (Fig. 1B-D). While, the actual mitochondrial damage was not shown.

Transfection efficiency of siDKK1 prior to RNA-seq. Following transfection with siDKK1, expression levels of DKK1 in HSMCs were significantly decreased (Fig. 2A), indicating that siDKK1 effectively reduced the expression of DKK1. Subsequently, cells were divided into four groups for RNA sequencing: NC, siDKK1, NC-Ang II and siDKK1-Ang II. Prior to sequencing, the expression levels of DKK1 were detected in samples. Results of the RT-qPCR revealed that the levels of DKK1 expression was significantly decreased in the Ang II stimulated group following transfection with siDKK1 (Fig. 2B).

DEGs analysis following DKK1 silencing. DEGs were analyzed using RNA-seq, and statistical analysis of DEGs are displayed in Fig. 3A; notably, 'up' is used to indicate genes that are upregulated in expression in the treatment group, compared with the control group, 'down' is used to indicate genes that are downregulated in expression in the treatment group, compared with the control group and total is used to indicate the total number of genes with significant differences between the two groups. According to the upregulated genes of each comparison group, a volcano map

of DEGs was produced (Fig. 3B). The volcano map of DEGs in NC-Ang II and NC groups is displayed in Fig. 3C. There were 1,143 genes upregulated and 1,198 genes downregulated. The volcano map of DEGs in siDKK1 and NC groups is displayed in Fig. 3D. There were 1,478 genes upregulated and 2,366 genes downregulated. The volcano map of DEGs in siDKK1-Ang II and NC-Ang II groups is displayed in Fig. 3E. There were 304 genes upregulated and 332 genes downregulated. Genes that were significantly upregulated, significantly downregulated or exhibited no significant differential expression were marked with different colors; blue indicated downregulation, whereas red indicated upregulation. Cluster heat maps of all DEGs were also established, and these are displayed in Fig. 3F. DEG clustering heat maps of NC-Ang II vs. NC, siDKK1 vs. NC and siDKK1-Ang II vs. NC-Ang II are displayed in Fig. 3G and I, respectively. Heat maps of all differentially expressed genes were drawn, including each biological repetition. Rows represent genes, columns represent groups for comparative analysis. Genes that were significantly upregulated or significantly downregulated were marked with different colors; blue indicated downregulation and red indicated upregulation. The clustering tree diagrams on the left and top show the similarities between genes or samples. The closer the branches, the closer the expression patterns.

GO and KEGG functional enrichment analysis. Results of the GO and KEGG functional enrichment analyses revealed that the top 600 DEGs of NC-Ang II vs. NC were associated with 'Negative regulation of the immune system process', 'Collagen-containing extracellular matrix', 'Extracellular matrix structural constituent' and 'Circadian entrainment' (Fig. 4A). Moreover, the top 600 DEGs of siDKK1 vs. NC were associated with 'Neutrophil extracellular trap formation', 'Negative regulation of viral genome replication', 'Protein-DNA complex' and 'Oxygen carrier activity' (Fig. 4B). Results of the present study also demonstrated that the top 600 DEGs of siDKK1-Ang II vs. NC-Ang II were associated with the 'Cytokine-cytokine receptor interaction', 'Defense response to virus', 'Collagen-containing extracellular matrix' and 'Unfolded protein binding' (Fig. 4C).

Key downstream genes following DKK1 silencing. A Venn diagram was used to identify 1,332 DEGs that were co-expressed across the different groups. The Venn diagram shows the intersection relationship of four groups of DEGs (NC-Ang II vs. NC, siDKK1 vs. NC, siDKK1-Ang II vs. NC-Ang II and siDKK1-Ang II vs. siDKK1). Each color represents one group. The number of DEGs co-expressed in all four groups was 1332 (Fig. 5A). Functional enrichment analyses using GO and KEGG revealed that the co-expressed DEGs were associated with 'Ribonucleoprotein complex biogenesis', 'Cell-substrate junction', 'Cadherin binding' and 'Protein processing in the endoplasmic reticulum' pathway (Fig. 5B). RRA analysis was performed using 1,332 co-expressed DEGs in all four groups in the aforementioned Venn diagram, and the top 20 genes obtained are displayed in Fig. 5C. The heat map analyzed using RRA revealed the Log₂ fold change value (Fig. 5D). Rows represent

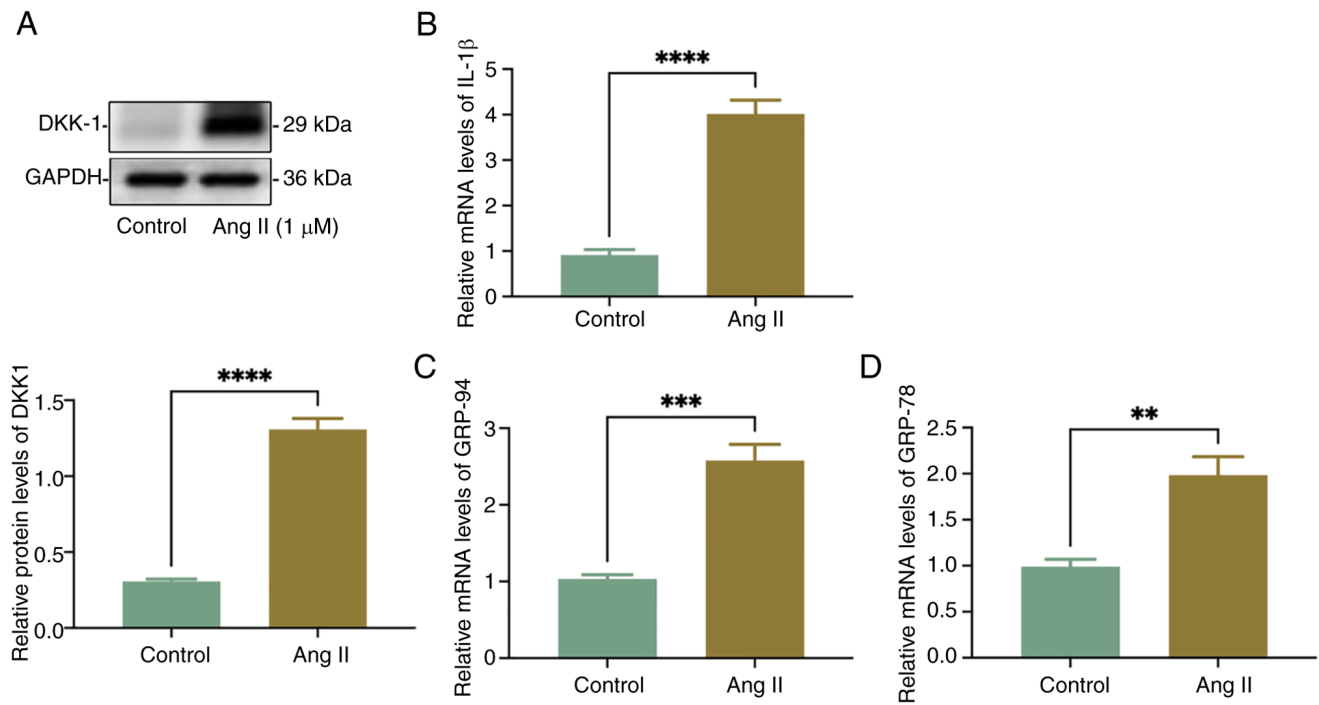


Figure 1. Ang II promotes DKK1 expression of HSMCs and mitochondrial damage. HSMCs treated with Ang II (1 μM) or without (control). (A) Western blotting revealed the DKK1 protein expression levels of HSMCs. (B) Reverse transcription-quantitative PCR results showed the mRNA expression level of IL-1β increases in HSMCs treated with Ang II. (C) Reverse transcription-quantitative PCR results showed the mRNA level of GRP-94 increases in HSMCs treated with Ang II. (D) Reverse transcription-quantitative PCR results showed the mRNA expression level of GRP-78 increases in HSMCs treated with Ang II. **P<0.01, ***P<0.001 and ****P<0.0001. Ang II, angiotensin II; HSMCs, human smooth muscle cells; DKK1, Dickkopf-1; IL, interleukin; GRP, glucose regulated protein.

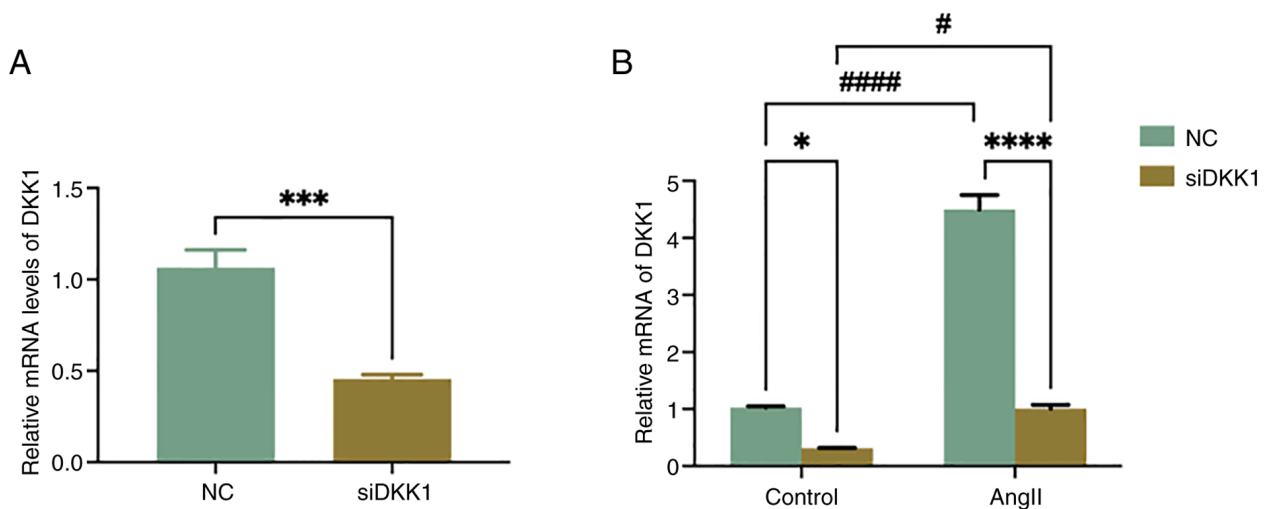


Figure 2. Transfection efficiency of siDKK1. (A) Reverse transcription-quantitative PCR results showed the mRNA expression level of DKK1 in siDKK1 and NC; (B) Reverse transcription-quantitative PCR results showed the mRNA expression level of DKK1 in each group. *P<0.05, ***P<0.001 and ****P<0.0001; #P<0.05 and ###P<0.0001. NC, negative control; siDKK1, small interfering RNA for DKK1; DKK1, Dickkopf-1; Ang II, angiotensin II.

genes, columns represent groups for comparative analysis. Genes that were significantly upregulated or significantly downregulated were marked with different colors; blue indicated downregulation and red indicated upregulation. Functional enrichment analysis using GO and KEGG demonstrated the potential association with ‘Negative regulation of viral genome replication’, ‘Endoplasmic reticulum lumen’ and ‘Coronavirus disease-COVID-19’

(Fig. 5E). Notably, SMDT1 was identified in the RRA analysis, this is a mitochondrial calcium ion regulatory protein and was therefore investigated further. Results of the RT-qPCR assay revealed that the mRNA expression levels of SMDT1 were increased 2.78-fold following Ang II stimulation. In addition, following DKK1 silencing, mRNA expression levels of SMDT1 were downregulated by 0.37-fold (Fig. 5F).

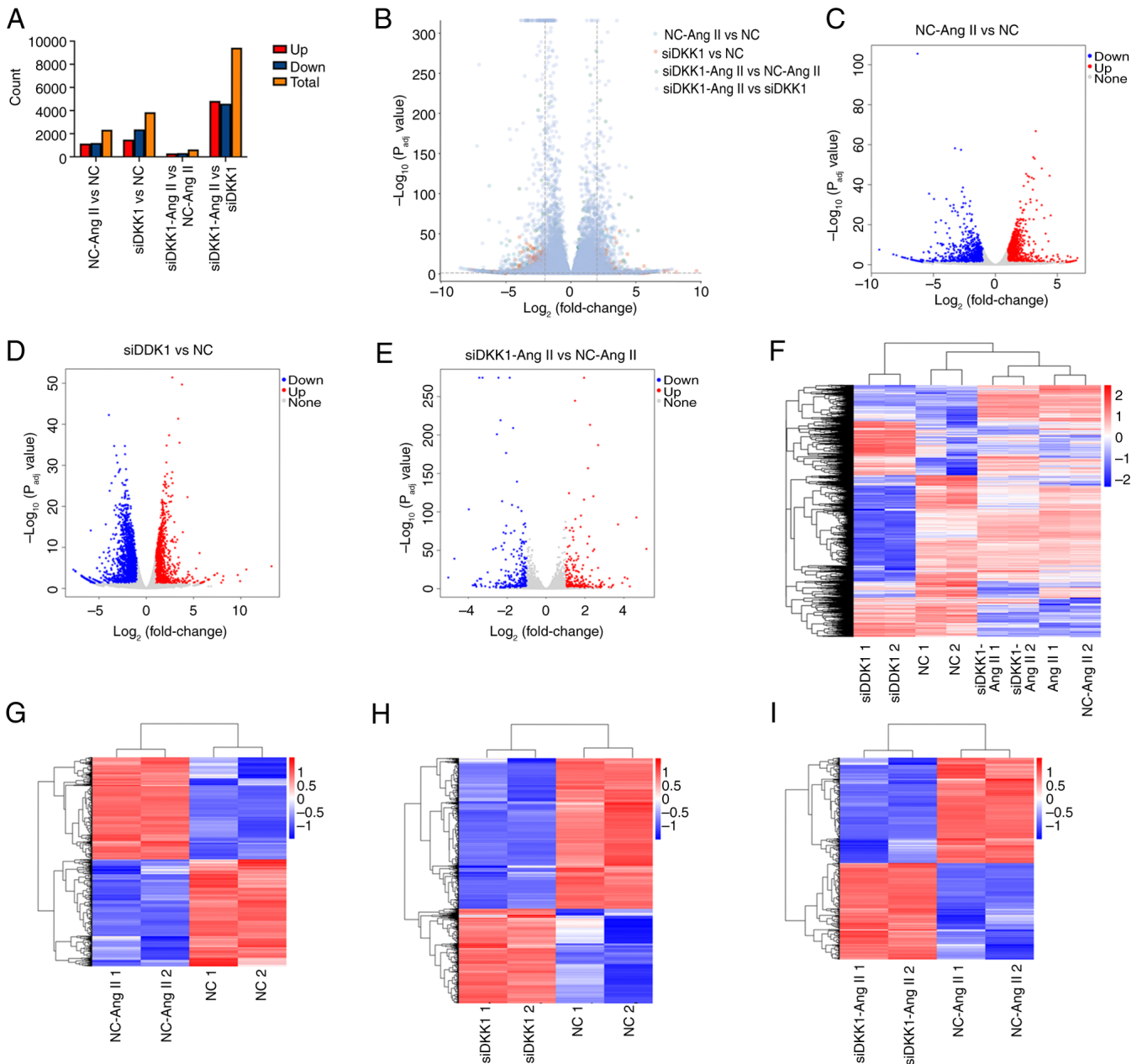


Figure 3. DEGs analysis after DKK1 silencing. (A) The distribution of DEGs. (B) Volcano map of all DEGs. (C) Volcano map of DEGs in NC-Ang II vs. NC. (D) Volcano map of DEGs in siDKK1 vs. NC. (E) Volcano map of DEGs in siDKK1-Ang II vs. NC-Ang II. (F) Clustering heat map of all DEGs. (G) Clustering heat map of DEGs in NC-Ang II vs. NC. (H) Clustering heat map of DEGs in siDKK1 vs. NC. (I) Clustering heat map of DEGs in siDKK1-Ang II vs. NC-Ang II. DEGs, differentially expressed genes; NC, treated with scrambled siRNAs as negative control; siDKK1, treated with siRNAs targeting human DKK1; Ang II, treated with Ang II (1 μ M). NC, negative control; siDKK1, small interfering RNA for DKK1; DKK1, Dickkopf-1; Ang II, angiotensin II.

Discussion

The present study aimed to elucidate the potential association between DKK1 and AAA. Following stimulation of Ang II in primary HSMCs, the results of the present study revealed that the expression of DKK1 in HSMCs was elevated. Following the successful knockdown of DKK1 using targeted siRNA, RNA-seq was used to further investigate the downstream DEGs. Results of RNA-seq and RT-qPCR analyses demonstrated that SMDT1 was significantly down-regulated following DKK1 silencing, indicating that DKK1 may participate in the Ang II-induced mitochondrial injury of HSMCs.

AAA is a complex pathological disease associated with the artery walls, and is a key cause of mortality in the elderly population, due to the rupture of dilated aorta tissue (3). Effective pharmacotherapies for halting the growth and rupture of AAA or delaying the requirement for surgical repair are lacking at present. Risk factors for this condition include smoking, obesity, aging, VSMC phenotype transitions, metabolic disorders, nuclear receptors, apoptosis and inflammation (1,8). Notably, progressive inflammation is the focus of numerous studies and is a well-established hallmark of AAA progression (28,29). Yuan *et al* (30) revealed that various inflammatory cell-associated mechanisms participate in AAA development, such as T cells, macrophages, dendritic cells,

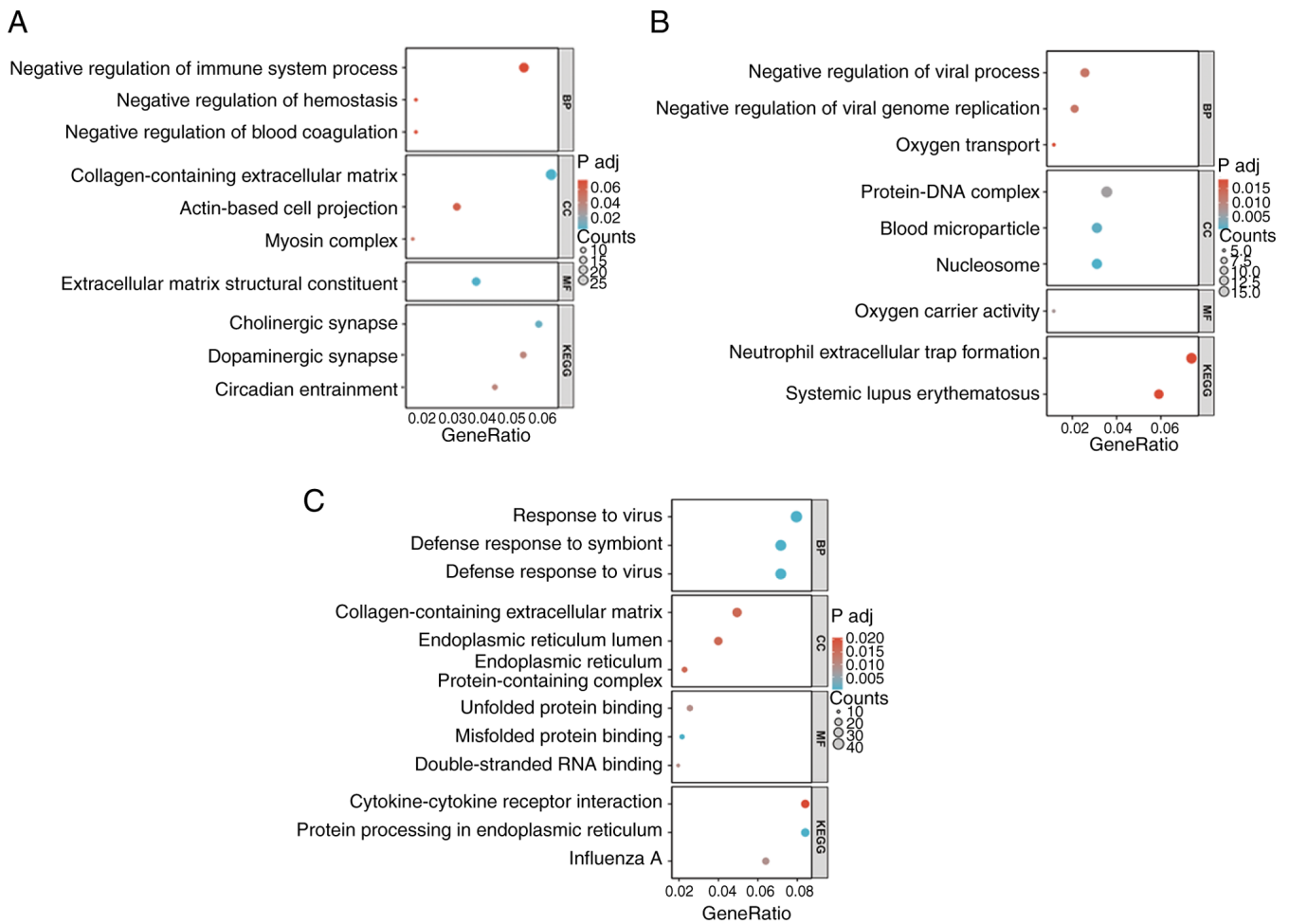


Figure 4. GO and KEGG functional enrichment analysis. (A) Functional enrichment analysis of GO and KEGG of DEGs in NC-Ang II vs. NC. (B) Functional enrichment analysis of GO and KEGG of DEGs in siDkk1 vs. NC. (C) Functional enrichment analysis of GO and KEGG of DEGs in siDkk1-Ang II vs. NC-Ang II. NC, treated with scrambled siRNAs as negative control; siDkk1, treated with siRNAs targeting human DKK1; Ang II, treated with Ang II (1 μ M). GO, gene ontology; KEGG, Kyoto Encyclopedia of Genes and Genomes; NC, negative control; siDkk1, small interfering RNA for DKK1; DKK1, Dickkopf-1; Ang II, angiotensin II; BP, biological processes; CC, cellular components; MF, molecular functions; P adj, adjusted P.

neutrophils, B cells and mast cells. Notably, AAA may begin with an immune response to various antigens within the aortic wall, which leads to the chemotaxis and infiltration of immune cells and, ultimately, the release of different cytokines. This may cause damage to the vascular endothelial cells and aggregation of platelets, leading to aortic dilation; notably, this process is comparable to the initiation of atherosclerosis (30). In addition, thrombosis may participate in the pathogenesis of AAA; results of a previous study revealed that a greater thrombus burden was associated with a higher rupture risk even at lower AAA diameters, which was strongly interconnected with inflammation and hemodynamics (31,32). The study showed that antithrombotic therapies could prevent and stabilize AAA; thus, the inhibition of platelets and coagulation factors may exhibit potential in reducing the risk of AAA development (31). However, further investigations are required to determine key biomarkers that may influence AAA pathogenesis, and to develop novel pharmacological strategies for the clinical management of AAA.

Biomarkers associated with cardiovascular disease may also exhibit potential as predictors for aortic disease, as atherosclerosis plays a key role in the progression of AAA (29).

Notably, atherosclerosis contributes to the progression of AAA in various ways, including the release of pro-inflammatory cytokines, shear stress and arterial remodeling. Thus, the regulation of atherosclerotic risk factors is of importance in patients with AAA (31), and aneurysms of the abdominal aorta represent a notable cardiovascular risk. A previous study revealed that the renin angiotensin system plays a key role in atherogenesis (33); notably, Ang II is an important active peptide of the renin angiotensin system, and is widely involved in the development of cardiovascular diseases, such as atherosclerosis and hypertension (34). Ang II may indirectly influence the atherogenic process via hemodynamic effects, as a result of increased arterial blood pressure. In addition, Ang II has also been shown to participate in the stimulation of monocyte recruitment, recruitment and activation of macrophages and enhanced oxidative stress, which are directly associated with the progression of atherogenesis; these factors are consistent with the chemoattractant property of Ang II (34).

Results of previous studies revealed the association between Ang II and the development of AAA. Blocking Ang II using either angiotensin-converting enzyme inhibitors or angiotensin receptor blockers was associated with a reduction

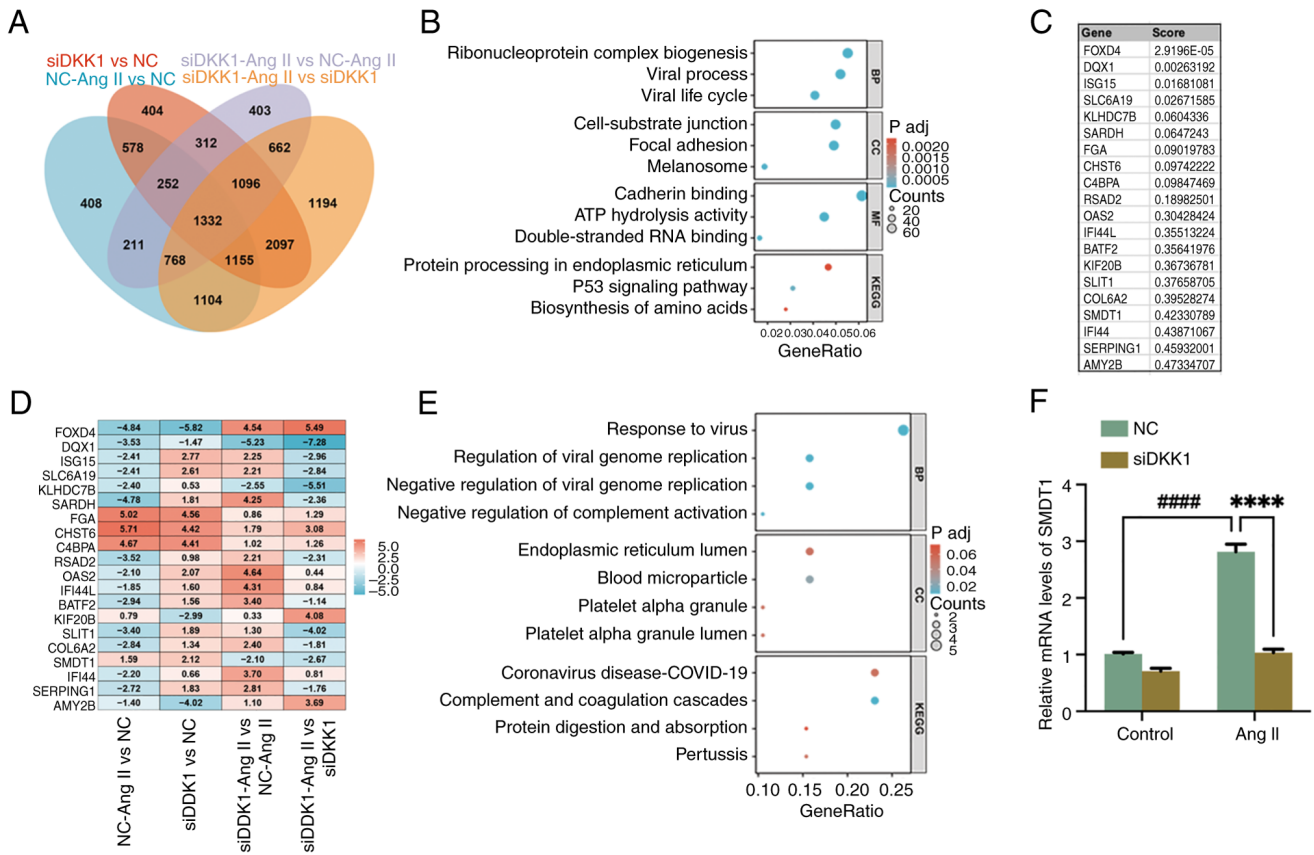


Figure 5. Identification of downstream key genes after DKK1 silencing. (A) Venn diagram showed co-expressed DEGs. (B) Functional enrichment analysis of GO and KEGG of co-expressing DEGs. (C) The top 20 genes in RRA analysis. (D) Heat map of RRA analysis. (E) Functional enrichment analysis of GO and KEGG of the top 20 genes in RRA analysis. (F) Reverse transcription-quantitative PCR results showed the mRNA expression level of SMDT1. **** $P < 0.0001$; #### $P < 0.0001$. NC, treated with scrambled siRNAs as negative control; siDDK1, treated with siRNAs targeting human DKK1; Ang II, treated with Ang II (1 μ M). GO, gene ontology; KEGG, Kyoto Encyclopedia of Genes and Genomes; NC, negative control; siDDK1, small interfering RNA for DKK1; DKK1, Dickkopf-1; Ang II, angiotensin II; BP, biological processes; CC, cellular components; MF, molecular functions; DEGS, differentially expressed genes; RRA, robust rank aggregation; SMDT1, single-pass membrane protein with aspartate rich tail 1.

of mortality in patients with AAA (34,35). Furthermore, within days of Ang II infusion into mice, medial accumulation of macrophages and elastin degradation in infrarenal aortic segments occur in the lesion of AAA (36). The characteristics of Ang II-induced AAA were comparable with those of atherosclerosis, such as activation of an inflammatory response, stimulation of metabolic disorders, nuclear receptors and apoptosis (34). Ang II infusion of Apo E^{-/-} mice is a widely established modeling method to induce AAA formation; in this model, an osmotic pump is inserted into hyperlipidemic mice to continually inject Ang II, this induces aneurysm phenotypes without surgical intervention (34,37). A key principle of the Ang II infusion model is systemic atherosclerosis, mobilization of systemic inflammation through changing the hemodynamics of mice and aggravation of artery wall damage to induce aneurysm formation. In the present study, to the best of our knowledge, for the first time HSMCs were stimulated with Ang II to mimic the pathological environment of AAA.

VSMCs are the main component of the blood vessel wall and exhibit numerous physiological functions, and the membrane of the blood vessel wall is mainly composed of VSMCs and extracellular matrix synthesized by VSMCs. In the pathological course of AAA, the release of MMPs produce high levels of ROS to damage VSMCs. VSMCs with oxidative

damage exhibit abnormal proliferation and apoptosis, promote the decline of elastin and collagen synthesis and lead to the degeneration or even rupture of the artery wall (38).

DKK1 is a conserved secreted glycoprotein that mediates endocytosis and regulates the activity of the Wnt signaling pathway through binding to LRP5/6, Kremen and other receptors on the cell membrane (14). Results of a previous study revealed that serum DKK1 plays an important role in the development of vascular diseases, such as coronary atherosclerosis and acute ischemic stroke (39). In 2009, Ueland *et al* (40) initially reported that patients with coronary artery disease or advanced carotid plaques exhibited increased levels of DKK1, both in serum and within the atherosclerotic lesion. DKK1 is involved in platelet-induced endothelial cell activation, and both endothelial and platelet-derived DKK1 could increase the inflammatory response between them; these results indicate that DKK1 may increase the inflammatory response in atherosclerotic plaques thus, playing a role in promoting atherosclerosis (40). Di *et al* (41) revealed that DKK1 overexpression led to the formation of enlarged and destabilized atherosclerotic lesions, high levels of apoptosis in the aorta and the development of carotid plaque. Moreover, DKK1-mediated apoptosis in human umbilical vein endothelial cells was promoted through activation of endoplasmic reticulum stress via the JNK

pathway and canonical Wnt signaling (41). Thus, DKK1 plays a key role as a biomarker during the pathological development of atherosclerosis, and is associated with inflammation facilitation, platelet activation and endothelial dysfunction. When exposed to atherogenic factors, such as oxidized low-density lipoprotein receptor or disturbed flow, platelets or endothelial cells release DKK1, resulting in vascular inflammation, endothelial-mesenchymal transition and apoptosis (17). In addition, DKK1 directly facilitates the expression of biomarkers that participate in the pathogenesis of atherosclerosis, such as plasminogen activator inhibitor type 1, clusterin/apolipoprotein J and pentraxin 3 (42). Results of previous studies demonstrated the association between DKK1 and mitochondrial disorders; DKK1 knockdown in human pulmonary artery endothelial cells cultured under hypoxic conditions increased the levels of ROS and the extent of mitochondrial DNA damage and inhibited mitochondrial membrane hyperpolarization (18,43). Moreover, DKK1 exacerbated doxorubicin-induced cardiomyocyte apoptosis and mitochondrial dysfunction (44). Studies focused on tumors revealed that DKK1 induced the apoptosis of JEG3 and BeWo trophoblastic tumor cells through the mitochondrial apoptotic pathway (45), and DKK1 may inhibit Wnt/Ca₂⁺-CaMKII-NF-κB signaling (46). Although DKK1 exhibits potential as a biomarker in cardiovascular disease, it is still unknown whether DKK1 is involved in the regulation of AAA. Further investigations into the potential role of DKK1 in AAA are required.

MCU complex consists of at least four main components: The pore-forming subunit (MCU) capable of higher-order oligomerization, the essential MCU regulator (EMRE) and two membrane gate-keeping factors (MICU1 and MICU2) (47,48). The molecular identification of MCU led to further studies focused on mitochondrial calcium homeostasis (49,50). Results of previous studies provided novel insights into the role of MCU in physiological and pathological events (51), including AAA. Hypertension, induced by chronic infusion of angiotensin II in the *Micu2*-depleted mice, led to a progressive increase in the aortic diameter and eventually to aneurysms (52). MCU dysfunction alters the dynamics of mitochondrial Ca²⁺, which in turn provokes pathological conditions affecting multiple organs, such as the heart, skeletal muscle and brain (53). MCU also plays key roles in the development of atherosclerosis, through modulating intracytoplasmic Ca²⁺ concentration; MCU inhibition improved impaired macrophage efferocytosis, and decreased ROS generation. Macrophage efferocytosis eliminated apoptotic cells and prevented the release of inflammatory factors and the formation of foam cells, thereby alleviating atherosclerosis (54). Moreover, Patel *et al* (55) revealed that different shear stress patterns in vascular endothelial cells modulated MCU complex subunit expression, which, in turn, impacted the pathological process of atherosclerosis.

SMDT1, a subunit of the MCU complex, essential for bridging the calcium-sensing role of MICU1 and MICU2, is involved in regulating calcium influx into the mitochondria of almost all mammalian tissues, which is of importance for regulating energy production and cell signaling due to ATP synthesis and apoptosis (56,57). SMDT1 variants impair EMRE-mediated mitochondrial calcium uptake in patients with muscle involvement (58). Results of a previous study

revealed that SMDT1 overexpression promoted mitochondrial fission in PDAC cells. SMDT1-driven change in mitochondrial dynamics morphology mediates apoptosis in pancreatic ductal adenocarcinoma (59).

A recent Mendelian randomization analysis revealed a causal association between elevated levels of SMDT1 and increased risks of cardiovascular disease, including coronary atherosclerosis, myocardial infarction and cardiomyopathy (60). In the present study, Ang II stimulated HSMCs to simulate AAA pathological damage, and following stimulation of Ang II, the concentration of DKK1 was increased and the expression levels of SMDT1 were increased concurrently. Notably, both DKK1 and SMDT1 levels were reduced following DKK1 silencing; thus, we hypothesize that DKK1/SMDT1 may participate in Ang II-induced mitochondrial injury of human smooth muscle cells, which may act as a novel pathological process in AAA.

Notably, the present study exhibits limitations. For example, only *in vitro* experiments were performed in the absence of *in vivo* validation, and only one cell type, namely HSMCs, were used, in the absence of endothelial/macrophage co-culturing. Therefore, the physiological relevance of these findings remains to be fully elucidated. The present study focused on understanding potential changes in the expression of downstream mitochondrial function-associated protein, SMDT1, following DKK1 silencing under Ang II stimulation. Further functional experiments are required.

To the best of our knowledge, the present study is the first to determine the role of DKK1/SMDT1 in AAA. In conclusion, the present study provided novel insights into the role of DKK1/SMDT1 in inflammatory responses in vascular diseases, which may aid in further understanding the pathophysiological mechanisms that are associated with AAA.

Acknowledgements

Not applicable.

Funding

The present study was funded by The Projects of Technological Innovation Development Program in Yantai City (grant no. 2022YD071), Traditional Chinese medicine science and technology project of Shandong Province (grant no. M-2023017), Binzhou Medical University research start-up fund (grant no. BY2020KJ46) and Introduction of Talent Research Initiation Fund of Central Hospital Affiliated to Shandong First Medical University (grant no. YJRC2022017).

Availability of data and materials

The data generated in the present study may be found in the National Center for Biotechnology Information under the login number of the data set: PRJNA1234348 or at the following URL: <http://www.ncbi.nlm.nih.gov/bioproject/1234348>.

Authors' contributions

XC, BY and ZL were responsible for performing the bioinformatics analysis using software. data collection,

statistical analysis and manuscript writing. ZG, PQ and XL helped with data collection, statistical analysis and literature search. LW and AL supervised the project and were involved in the study design, data analysis and writing of the manuscript. LW and AL confirm the authenticity of all the raw data. All authors have read and approved the final manuscript.

Ethics approval and consent to participate

Not applicable.

Patient consent for publication

Not applicable.

Competing interests

The authors declare that they have no competing interests.

References

- Ullery BW, Hallett RL and Fleischmann D: Epidemiology and contemporary management of abdominal aortic aneurysms. *Abdom Radiol (NY)* 43: 1032-1043, 2018.
- Kent KC: Clinical practice. Abdominal aortic aneurysms. *N Engl J Med* 371: 2101-2108, 2014.
- Zhao G, Fu Y, Cai Z, Yu F, Gong Z, Dai R, Hu Y, Zeng L, Xu Q and Kong W: Unspliced XBP1 confers VSMC homeostasis and prevents aortic aneurysm formation via FoxO4 interaction. *Circ Res* 121: 1331-1345, 2017.
- Li Y, Ren P, Dawson A, Vasquez HG, Ageedi W, Zhang C, Luo W, Chen R, Li Y, Kim S, *et al*: Single-cell transcriptome analysis reveals dynamic cell populations and differential gene expression patterns in control and aneurysmal human aortic tissue. *Circulation* 142: 1374-1388, 2020.
- Wang H, Kazaleh M, Gioscia-Ryan R, Millar J, Temprano-Sagrera G, Wood S, Van Den Bergh F, Blin MG, Wragg KM, Luna A, *et al*: Deficiency of mitophagy mediator Parkin in aortic smooth muscle cells exacerbates abdominal aortic aneurysm. *bioRxiv [Preprint]*: 2024.10.30.621201, 2025.
- Sun LY, Lyu YY, Zhang HY, Shen Z, Lin GQ, Geng N, Wang YL, Huang L, Feng ZH, Guo X, *et al*: Nuclear receptor NR1D1 regulates abdominal aortic aneurysm development by targeting the mitochondrial tricarboxylic acid cycle enzyme aconitase-2. *Circulation* 146: 1591-1609, 2022.
- Tavris BS, Peters AS, Böckler D and Dihlmann S: Mitochondrial dysfunction and increased DNA damage in vascular smooth muscle cells of abdominal aortic aneurysm (AAA-SMC). *Oxid Med Cell Longev* 2023: 6237960, 2023.
- Liu Y, Yu M, Wang H, Dorsey KH, Cheng Y, Zhao Y, Luo Y, Zhao G, Zhao Y, Lu H, *et al*: restoring vascular smooth muscle cell mitochondrial function attenuates abdominal aortic aneurysm in mice. *Arterioscler Thromb Vasc Biol* 45: 523-540, 2025.
- Azhdari M and Zur Hausen A: Wnt/ β -catenin and notch signaling pathways in cardiovascular disease: Mechanisms and therapeutic approaches. *Pharmacol Res* 211: 107565, 2025.
- Methatham T, Tomida S, Kimura N, Imai Y and Aizawa K: Inhibition of the canonical Wnt signaling pathway by a β -catenin/CBP inhibitor prevents heart failure by ameliorating cardiac hypertrophy and fibrosis. *Sci Rep* 11: 14886, 2021.
- Rong Z, Li F, Zhang R, Niu S, Di X, Ni L and Liu C: Ant-neointimal formation effects of SLC6A6 in preventing vascular smooth muscle cell proliferation and migration via Wnt/ β -catenin signaling. *Int J Mol Sci* 24: 2018, 2023.
- Schunk SJ, Floege J, Fliser D and Speer T: WNT- β -catenin signalling-a versatile player in kidney injury and repair. *Nat Rev Nephrol* 17: 172-184, 2021.
- Xu L, Liu B, Ma H, Qi E, Ma J, Chang T, Zhang J, Zhang W, Chen W, Cao X and Xiong X: O-GlcNAc transferase promotes vascular smooth muscle calcification through modulating Wnt/ β -catenin signaling. *Faseb J* 38: e70271, 2024.
- Boucher P, Matz RL and Terrand J: atherosclerosis: Gone with the Wnt? *Atherosclerosis* 301: 15-22, 2020.
- Klingenschmid G, Tschiederer L, Himmler G, Rungger G, Brugger S, Santer P, Willeit J, Kiechl S and Willeit P: Associations of serum dickkopf-1 and sclerostin with cardiovascular events: results from the prospective bruneck study. *J Am Heart Assoc* 9: e014816, 2020.
- Xu H, Ding Z, Chen J, Zhang Y, Shan W, Chen X, Liu X, Gao Y and Han G: Correlation between serum Dickkopf-1 (DKK1) levels and coronary artery stenosis. *Nutr Metab Cardiovasc Dis* 33: 168-176, 2023.
- Baetta R and Banfi C: Dkk (dickkopf) proteins. *Arterioscler Thromb Vasc Biol* 39: 1330-1342, 2019.
- Wang Q, Tian J, Li X, Liu X, Zheng T, Zhao Y, Li X, Zhong H, Liu D, Zhang W, *et al*: Upregulation of endothelial DKK1 (dickkopf 1) promotes the development of pulmonary hypertension through the spl1 (specificity protein 1)/SHMT2 (serine hydroxymethyltransferase 2) pathway. *Hypertension* 79: 960-973, 2022.
- Huo C, Liu Y, Li X, Xu R, Jia X, Hou L and Wang X: LRRC8A contributes to angiotensin II-induced cardiac hypertrophy by interacting with NADPH oxidases via the C-terminal leucine-rich repeat domain. *Free Radic Biol Med* 165: 191-202, 2021.
- Livak KJ and Schmittgen TD: Analysis of relative gene expression data using real-time quantitative PCR and the 2(-Delta Delta C(T)) method. *Methods* 25: 402-408, 2001.
- Martin M: Cutadapt removes adapter sequences from high-throughput sequencing reads. *EMBnet J* 17: 3, 2011.
- Stark R, Grzelak M and Hadfield J: RNA sequencing: The teenage years. *Nat Rev Genet* 20: 631-656, 2019.
- Wickham H: ggplot2: Elegant graphics for data analysis. New York, NY, Springer, 2009.
- Chen H and Boutros PC: VennDiagram: A package for the generation of highly-customizable Venn and Euler diagrams in R. *BMC Bioinformatics* 12: 35, 2011.
- Kolde R, Laur S, Adler P and Viljo J: Robust rank aggregation for gene list integration and meta-analysis. *Bioinformatics* 28: 573-580, 2012.
- Yu G, Wang LG, Han Y and He QY: clusterProfiler: An R package for comparing biological themes among gene clusters. *OMICS* 16: 284-287, 2012.
- Szklarczyk D, Gable AL, Nastou KC, Lyon D, Kirsch R, Pyysalo S, Doncheva NT, Legeay M, Fang T, Bork P, *et al*: The STRING database in 2021: Customizable protein-protein networks, and functional characterization of user-uploaded gene/measurement sets. *Nucleic Acids Res* 49 (D1): D605-D612, 2021.
- Trollope AF and Golledge J: Angiopoietins, abdominal aortic aneurysm and atherosclerosis. *Atherosclerosis* 214: 237-243, 2011.
- Khan H, Abu-Raisi M, Feasson M, Shaikh F, Saposnik G, Mamdani M and Qadura M: Current prognostic biomarkers for abdominal aortic aneurysm: A comprehensive scoping review of the literature. *Biomolecules* 14: 661, 2024.
- Yuan Z, Lu Y, Wei J, Wu J, Yang J and Cai Z: Abdominal aortic aneurysm: Roles of inflammatory cells. *Front Immunol* 11: 609161, 2021.
- Bontekoe J, Matsumura J and Liu B: Thrombosis in the pathogenesis of abdominal aortic aneurysm. *JVS Vasc Sci* 4: 100106, 2023.
- Liu X, Weng Y, Lou J, Chen X, Du C and Tang L: Combinational therapy with aspirin and ticagrelor alleviates vascular inflammation and angiotensin II-driven abdominal aortic aneurysm formation in mice. *Austin J Cardiovasc Dis Atherosclerosis* 9: 1048, 2022.
- Lu H, Rateri DL, Bruemmer D, Cassis LA and Daugherty A: Involvement of the renin-angiotensin system in abdominal and thoracic aortic aneurysms. *Clin Sci (Lond)* 123: 531-543, 2012.
- Daugherty A, Manning MW and Cassis LA: Angiotensin II promotes atherosclerotic lesions and aneurysms in apolipoprotein E-deficient mice. *J Clin Invest* 105: 1605-1612, 2000.
- Kristensen KE, Torp-Pedersen C, Gislason GH, Egffjord M, Rasmussen HB and Hansen PR: Angiotensin-converting enzyme inhibitors and angiotensin II receptor blockers in patients with abdominal aortic aneurysms: Nation-wide cohort study. *Arterioscler Thromb Vasc Biol* 35: 733-740, 2015.
- Daugherty A and Cassis LA: Mouse models of abdominal aortic aneurysms. *Arterioscler Thromb Vasc Biol* 24: 429-434, 2004.
- Sawada H, Lu HS, Cassis LA and Daugherty A: Twenty years of studying AngII (angiotensin II)-induced abdominal aortic pathologies in mice: Continuing questions and challenges to provide insight into the human disease. *Arterioscler Thromb Vasc Biol* 42: 277-288, 2022.
- Quintana RA and Taylor WR: Cellular mechanisms of aortic aneurysm formation. *Circ Res* 124: 607-618, 2019.

39. Zhu Z, Guo D, Zhong C, Wang A, Xie X, Xu T, Chen CS, Peng Y, Peng H, Li Q, *et al*: Serum Dkk-1 (dickkopf-1) Is a potential biomarker in the prediction of clinical outcomes among patients with acute ischemic stroke. *Arterioscler Thromb Vasc Biol* 39: 285-293, 2019.
40. Ueland T, Otterdal K, Lekva T, Halvorsen B, Gabrielsen A, Sandberg WJ, Paulsson-Berne G, Pedersen TM, Folkersen L, Gullestad L, *et al*: Dickkopf-1 enhances inflammatory interaction between platelets and endothelial cells and shows increased expression in atherosclerosis. *Arterioscler Thromb Vasc Biol* 29: 1228-1234, 2009.
41. Di M, Wang L, Li M, Zhang Y, Liu X, Zeng R, Wang H, Chen Y, Chen W, Zhang Y and Zhang M: Dickkopf1 destabilizes atherosclerotic plaques and promotes plaque formation by inducing apoptosis of endothelial cells through activation of ER stress. *Cell Death Dis* 8: e2917, 2017.
42. Magrini E, Mantovani A and Garlanda C: The dual complexity of PTX3 in health and disease: A balancing Act? *Trends Mol Med* 22: 497-510, 2016.
43. Kim IG, Kim SY, Kim HA, Kim JY, Lee JH, Choi SI, Han JR, Kim KC and Cho EW: Disturbance of DKK1 level is partly involved in survival of lung cancer cells via regulation of ROMO1 and γ -radiation sensitivity. *Biochem Biophys Res Commun* 443: 49-55, 2014.
44. Liang L, Tu Y, Lu J, Wang P, Guo Z, Wang Q, Guo K, Lan R, Li H and Liu P: Dkk1 exacerbates doxorubicin-induced cardiotoxicity by inhibiting the Wnt/ β -catenin signaling pathway. *J Cell Sci* 132: jcs228478, 2019.
45. Cui H, Li H, Li QL, Chen J, Na Q and Liu CX: Dickkopf-1 induces apoptosis in the JEG3 and BeWo trophoblast tumor cell lines through the mitochondrial apoptosis pathway. *Int J Oncol* 46: 2555-2561, 2015.
46. Zhuang X, Zhang H, Li X, Li X, Cong M, Peng F, Yu J, Zhang X, Yang Q and Hu G: Differential effects on lung and bone metastasis of breast cancer by Wnt signalling inhibitor DKK1. *Nat Cell Biol* 19: 1274-1285, 2017.
47. Oxenoid K, Dong Y, Cao C, Cui T, Sancak Y, Markhard AL, Grabarek Z, Kong L, Liu Z, Ouyang B, *et al*: Architecture of the mitochondrial calcium uniporter. *Nature* 533: 269-273, 2016.
48. Wang Y, Nguyen NX, She J, Zeng W, Yang Y, Bai XC and Jiang Y: Structural mechanism of EMRE-dependent gating of the human mitochondrial calcium uniporter. *Cell* 177: 1252-1261.e13, 2019.
49. Patron M, Granatiero V, Espino J, Rizzuto R and De Stefani D: MICU3 is a tissue-specific enhancer of mitochondrial calcium uptake. *Cell Death Differ* 26: 179-195, 2019.
50. Shamseldin HE, Alasmari A, Salih MA, Samman MM, Mian SA, Alshidi T, Ibrahim N, Hashem M, Faqeih E, Al-Mohanna F and Alkuraya FS: A null mutation in MICU2 causes abnormal mitochondrial calcium homeostasis and a severe neurodevelopmental disorder. *Brain* 140: 2806-2813, 2017.
51. Murgia M and Rizzuto R: Molecular diversity and pleiotropic role of the mitochondrial calcium uniporter. *Cell Calcium* 58: 11-17, 2015.
52. Tarasova NV, Vishnyakova PA, Logashina YA and Elchaninov AV: Mitochondrial calcium uniporter structure and function in different types of muscle tissues in health and disease. *Int J Mol Sci* 20: 4823, 2019.
53. Alevriadou BR, Patel A, Noble M, Ghosh S, Gohil VM, Stathopoulos PB and Madesh M: Molecular nature and physiological role of the mitochondrial calcium uniporter channel. *Am J Physiol Cell Physiol* 320: C465-C482, 2021.
54. Lu N, Zhu JF, Lv HF, Zhang HP, Wang PL, Yang JJ and Wang XW: Modulation of oxidized low-density lipoprotein-affected macrophage efferocytosis by mitochondrial calcium uniporter in a murine model. *Immunol Lett* 263: 14-24, 2023.
55. Patel A, Pietromicca JG, Venkatesan M, *et al*: Modulation of the mitochondrial Ca(2+) uniporter complex subunit expression by different shear stress patterns in vascular endothelial cells. *Physiol Rep* 11: e15588, 2023.
56. Sancak Y, Markhard AL, Kitami T, Kovács-Bogdán E, Kamer KJ, Udeshi ND, Carr SA, Chaudhuri D, Clapham DE, Li AA, *et al*: EMRE is an essential component of the mitochondrial calcium uniporter complex. *Science* 342: 1379-1382, 2013.
57. Arduino DM, Goh V, Mokranjac D and Perocchi F: Drug discovery assay to identify modulators of the mitochondrial Ca²⁺ uniporter. *Methods Mol Biol* 2277: 69-89, 2021.
58. Bulthuis EP, Adjobo-Hermans MJW, de Potter B, Hoogstraten S, Wezendonk LHT, Tutakhel OAZ, Wintjes LT, van den Heuvel B, Willems PHGM, Kamsteeg EJ, *et al*: SMDT1 variants impair EMRE-mediated mitochondrial calcium uptake in patients with muscle involvement. *Biochim Biophys Acta Mol Basis Dis* 1869: 166808, 2023.
59. Xie KF, Guo DD and Luo XJ: SMDT1-driven change in mitochondrial dynamics mediate cell apoptosis in PDAC. *Biochem Biophys Res Commun* 511: 323-329, 2019.
60. Meng H, He Y, Rui Y, Cai M, Fu D, Bi W, Luo B and Gao Y: Genetic predisposition and mitochondrial dysfunction in sudden cardiac death: Role of MCU complex genetic variations. *Cells* 14: 728, 2025.



Copyright © 2026 Chang et al. This work is licensed under a Creative Commons Attribution-NonCommercial-NoDerivatives 4.0 International (CC BY-NC-ND 4.0) License.